Finite element modeling of polyethylene pipe in dense sand subjected to lateral force

Saifa Anzum[1], Auchib Reza[1] & Ashutosh Sutra Dhar[1]
[1]Department of Civil Engineering – Memorial University of Newfoundland, St. John's, NL, Canada

GeoCalgary 2022 October 2-5 Reflection on Resources

ABSTRACT
Over the years, different experimental and numerical studies were conducted to understand the soil-pipe interaction for pipelines encountering ground movements focusing on steel pipes. Limited experimental studies were also conducted to examine the response of polyethylene pipes exposed to axial and lateral ground movements. This research focuses on developing a numerical modeling technique to simulate the experiments conducted at the Memorial University of Newfoundland on lateral ground movement effects on medium-density polyethylene (MDPE) pipes. The study simulates the test results with a nonlinear three-dimensional finite element (FE) model by idealizing soil behavior with the conventional Mohr-Coulomb (MC) model and stress-dependent soil properties, such as modulus of elasticity, the internal friction angle, and the dilation angle. The geometric nonlinearity was considered to account for the large deformation effects due to the ground deformations. The proposed techniques successfully simulated the load-displacement responses and the pipe's axial strains measured during multiple tests.

RÉSUMÉ
Au fil des ans, différentes études expérimentales et numériques ont été menées pour comprendre l'interaction sol-conduite pour les pipelines rencontrant des mouvements de terrain en se concentrant sur les conduites en acier. Des études expérimentales limitées ont également été menées pour examiner la réponse des conduites en polyéthylène exposées aux mouvements axiaux et latéraux du sol. Cette recherche porte sur le développement d'une technique de modélisation numérique pour simuler les expériences menées à l'Université Memorial de Terre-Neuve sur les effets du mouvement latéral du sol sur les tuyaux en polyéthylène à densité moyenne (MDPE). L'étude simule les résultats des tests avec un modèle d'éléments finis (FE) tridimensionnel non linéaire en idéalisant le comportement du sol avec le modèle conventionnel de Mohr-Coulomb (MC) et les propriétés du sol dépendantes de la contrainte, telles que le module d'élasticité, l'angle de frottement interne. , et l'angle de dilatation. La non-linéarité géométrique a été considérée pour tenir compte des grands effets de déformation dus aux déformations du sol. Les techniques proposées ont simulé avec succès les réponses charge-déplacement et les déformations axiales du tuyau mesurées au cours de plusieurs essais.

1 INTRODUCTION

Polyethylene pipes have been widely used in gas distribution systems since it was initially introduced to transport natural gas in the 1960s. It offers several benefits, including better corrosion resistance, the convenience of installation, and affordability. However, natural or artificial hazards could damage these pipes to the extent that the pipe's structural integrity is compromised. Geotechnical factors, however, have the most detrimental and long-term influence on the pipelines. Pipelines subjected to the ground movements have a complex interaction with the soil around them that is influenced by the direction of the ground movements and the boundary conditions of the pipe. The lateral and vertical ground movements are critically important among all these ground movements because they cause curvature and bending strain on pipes affecting internal soil-pipe friction (Hsu, 1993). Assessing the impact of ground movements on pipeline performance is essential for pipeline integrity assessment.

The early studies mainly focused on analyzing the lateral load impact on pipeline behavior by investigating anchor plates, retaining walls, and laterally loaded piles (Hansen, 1961; Ovesen, 1964; Ovesen and Strømann, 1972; Neely et al., 1973; Das and Seeley, 1975; Murray and Geddes, 1989). The experimental studies over the years predicted a wide range of maximum soil forces due to relative pipe–soil movement depending on multiple variables, such as material properties, boundary constraints, and loading rate. Studies on pipe underground deformations were conducted by Audibert and Nyman (1977), Trautmann (1983), Hsu (1993) and Konuk et al. (1999) through full-scale testing. They proposed some fundamental relationships between soil and pipe due to ground deformation in various directions. These works on investigating pipelines subjected to a ground movement were focused on examining the maximum lateral loads imposed on rigid pipes only. Almahakeri et al. (2012, 2014) conducted tests with steel pipes and Glass Fiber Reinforced Polymer (GFRP). Alarifi et al. (2021) recently conducted large-scale tests to investigate the lateral pipeline–soil interaction in sandy soil for polyethylene pipes. Although full-scale laboratory testing and field investigation are great for studying overall impacts on pipes, numerical models are generally cost-effective and faster. The numerical models can also be calibrated using data from physical testing to undertake parametric studies based on different material and geometric features.

Researchers conducted two-dimensional (2D) and three-dimensional (3D) lateral pullout numerical analyses

to validate the laboratory pullout test results on different types of pipes using various numerical modeling software. Popescu et al. (2001) conducted a 2D plane strain numerical analysis with a non-associated Mohr-Coulomb material model using Abaqus/Standard, which reasonably simulated the pre-peak behavior of dense sand. Yimsiri et al. (2004), Guo and Stolle (2005), and Roy et al. (2015) numerically analyzed the ground movement effect on buried pipelines under two-dimensional plane strain conditions. Several other 2D FE analyses are available (e.g., Daiyan et al., 2010; Jung et al., 2013 and Almahakeri et al., 2016), focusing on rigid pipes. However, the 2D Plane strain analysis is often inappropriate for analyzing soil-pipe interaction where the load transfer mechanism is non-uniform over the pipe length.

Studies were conducted using 3D finite element modeling to simulate buried polyethylene pipe behavior (e.g., Xie et al., 2013; Robert et al., 2016; Almahakeri et al., 2019). As the polyethylene pipes are flexible with a lower stiffness modulus, they show very different loading mechanisms than the rigid pipes. Therefore, more attention is required to analyze polyethylene pipe problems in 3D FE analyses.

Natural gas distribution pipes are often coupled with lateral branches or connections to distribute natural gas to the community members. If these pipe systems are exposed to landslides, the excessive bending strain or axial force induced at the joints can cause failure to the system by leakage, rupture, or joint failure. No study is currently available to assess the bending strain on a pipe and the axial force on the branch. Moreover, relatively limited information is available in the published literature on the flexural behavior of MDPE gas distribution pipes.

In this study, 3D FE analyses are performed to simulate pipe-soil interaction for MDPE pipes near a branch under the effects of lateral ground movement. The model was validated using the test data found from a series of full-scale laboratory tests conducted on MDPE pipes at Memorial University (Sinha et al., 2021). Then, the model was used to investigate the axial strain and the deformed shape at different pipe locations. Additionally, a parametric study is performed to provide deeper insight into the pipe response associated with higher burial depth ratios which could not be explored experimentally due to the design limitation of the test facility.

2 TESTING PROGRAM

The investigation of MDPE pipes under lateral ground movements was conducted by Sinha (2021) using a full-scale pipe testing facility developed at the Memorial University of Newfoundland, St. John's, NL. The soil movement near a pipe connection was considered, idealizing the system as shown in Figure 1. Figure 1(a) presents the ground movement phenomenon. The relative movement between the pipe and surrounding soil was simulated by pulling the buried pipe at the branch while the soil was fixed in the test cell (Figure 1b).

Four tests were performed on pipes with 42.2-mm (Tests T-1 and T-2) and 60-mm (Tests T-3 and T-4) diameters (thickness respectively 4.22 mm and 5.48 mm) and 1800 mm long, buried in dense sand. The test cell has plan dimensions of 4 m × 2 m and is 1.5 m deep, with steel walls. Above the pipe springline, soil cover was maintained at 337 mm (in test T-1), 480 mm (in test T-3) and 600 mm (in tests T-2 and T-4). The pipes were pulled by a cable through a hydraulic actuator at a 0.5 mm/min pulling rate during the tests. Additional details on the tests are available in Sinha (2021).

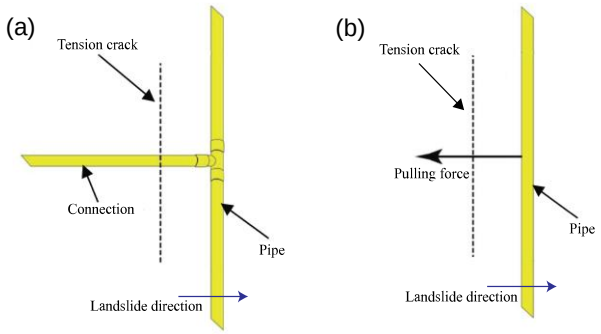

Figure 1. Pipe condition and test idealization (Sinha et al., 2021): (a) Pipe with lateral connection, (b) Test idealization

3 FINITE ELEMENT MODELING

Three-dimensional FE modeling was adopted to simulate the experimental setup using the commercial software package Abaqus (version 2019) (Dassault Systems 2019). The aim of the analysis is to establish the triaxial pipe–soil interaction using the conventional continuum-based methods to capture the peak forces mobilized in the soil and associated pipe strains at different locations.

3.1 Constitutive Model

The present investigation used the conventional elastic-perfectly plastic Mohr-Coulomb (MC) model to simulate the soil behavior. The Young's modulus (E_s) of soil was determined using Janbu's nonlinear model for a stress-dependent modulus of elasticity. The initial tangent modulus of elasticity, $E_{s,}$ is shown in Eq. (1).

$$E_S = K p_a \left(\frac{p'}{p_a}\right)^n \quad [1]$$

Where p_a is the atmospheric pressure (101.3 kPa); the Janbu model parameters n and K were considered as 0.5 and 150, respectively, as per Roy et al. (2018); p' is the mean effective confining pressure calculated from the following relation (Eq. 2).

$$p' = K_0 \gamma H \quad [2]$$

Where K_0 is the coefficient of lateral earth pressure at rest, γ is the unit weight of soil, and H is the depth of soil cover up to the springline level of the pipe. The Poisson's ratio of the soil was assumed to be 0.3. A nominal value of cohesion of 0.10 kPa was employed for numerical stability.

The parameters used to model the soil domain are summarized in Table 1.

The peak internal friction angle (ϕ_p') and dilation angle (ψ) have a significant influence on the load-displacement behavior of the soil-pipe system. The value of the peak friction angle is considerably affected by the level of stress and the density based on Bolton's empirical relation (Bolton, 1986) (Eq. 3).

$$\phi'_{\mathrm{p}} = \phi'_{\mathrm{c}} + 3D_r(10 - \ln p') \quad [3]$$

where D_r = the relative density; p' = mean effective stress; ϕ'_c = critical friction angle. Bolton's correlation is generally applicable at higher stress levels. However, the soil stress levels during the tests were relatively low. Ansari et al. (2018) provided a relationship for the direct shear test peak friction angle ($\phi'^{\,\mathrm{DS}}$) at a relatively low-stress level for dense sand (Eq. 4).

$$\phi'^{\,\mathrm{DS}} = -3.63 \times \ln p' + 49.19 \quad [4]$$

Table 1. Properties of sand

Parameters	Values			
	T-1	T-2	T-3	T-4
Initial Modulus of elasticity, E_s, (MPa)	4	5	4.5	5
Poisson's ratio, ν	0.3			
Density, ρ_s (kg/m^3)	1733			
Cohesion, c (kPa)	0.1			
Critical friction angle, ϕ_c' (°)	35			
Peak friction angle, ϕ_p' (°)	42	40	41	40
Dilation angle, ψ (°)	14	10	12	10

Lings and Dietz (2004) showed a relation between the peak friction angle of soil ($\phi'^{\,\mathrm{PS}}$) at plane strain condition and that found from the direct shear test ($\phi'^{\,\mathrm{DS}}$) which is $\phi'^{\,\mathrm{PS}} \approx \phi'^{\,\mathrm{DS}} + 5°$. According to Kulhawy and Mayne (1990), the $\phi'^{\,\mathrm{PS}}$ at plane strain condition is approximately 10 to 20% higher than the peak friction angle of soil ($\phi'^{\,\mathrm{TX}}$) at the triaxial condition for dense sand.

As the current study is performed for triaxial conditions, the $\phi'^{\,\mathrm{TX}}$ was used in the analysis. Based on effective normal stress, the peak friction angles were estimated to range between 42° and 40°. The dilation angle was estimated based on $\phi_p' = \phi_c' + 0.5\psi$ (Bolton, 1986). Figure 2 shows a comparison of the peak friction and dilation angles under conditions and those used in the current study.

For the MDPE pipe material, an isotropic elastic-plastic model was used. Das and Dhar (2021) reported that the stress-strain responses of MDPE pipe material are highly nonlinear and strain rate-dependent. A modified hyperbolic model, proposed by Suleiman and Coree (2004), was used to account for the strain rate-dependent behavior of polyethylene pipe material, as shown in Eq. (5).

$$\sigma = E_p\left(\frac{\varepsilon}{1+\eta\varepsilon}\right) \quad [5]$$

Where E_p is the initial Young's modulus, and η is a hyperbolic constant. These strain rate-dependent parameters can be obtained using the following equations

$$E_p = a(\dot{\varepsilon})^b \quad [6]$$

$$\eta = \frac{a(\dot{\varepsilon})^b}{c + d\ln(\dot{\varepsilon})} \quad [7]$$

where a, b, c, and d are model parameters, and $\dot{\varepsilon}$ is the strain rate. The strain rate during the tests was close to 10^{-5}/sec. The true stress-strain relation of pipe material corresponding to this strain rate was provided as the input for the FE analysis. Using the calculated parameters by Das and Dhar (2021), the initial modulus of elasticity is found as 413 MPa. The Poisson's ratio and density of the MDPE pipe are 0.46 and 940 kg/m^3, respectively.

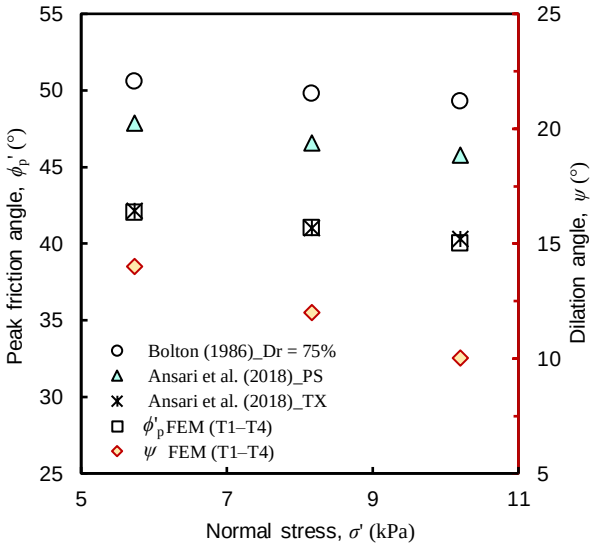

Figure 2. Peak friction angle and dilation angle based on effective stress

3.2 Model Geometry and Element Type

Figure 3 shows the geometry of the FE model considered. Although the tests were conducted in the 4 m long test facility, the soil behind the pulling direction has a negligible effect on the soil resistance. Therefore, only 0.5 m of soil behind the pipe pulling direction was modelled to increase computational efficiency. The soil length in front of the pipe was the same as that used during the tests (i.e., 2 m). The

width and depth of the soil were the same as those of the test facility. The width was 2 m, and the depth was varied according to the test embedment ratio. The pipe geometries were the same as those of the test pipes.

Eight-node solid linear hexahedral elements in reduced integration and hourglass control (C3D8R in Abaqus) were used to simulate the buried pipe and the surrounding soil domain. Though these lower-order (linear) elements are overly stiff due to shear locking, reduced integration and extremely fine meshes at the zone of interest prevented this volumetric locking issue. Therefore, reduced integration and extremely fine meshes at the zone of interest were employed.

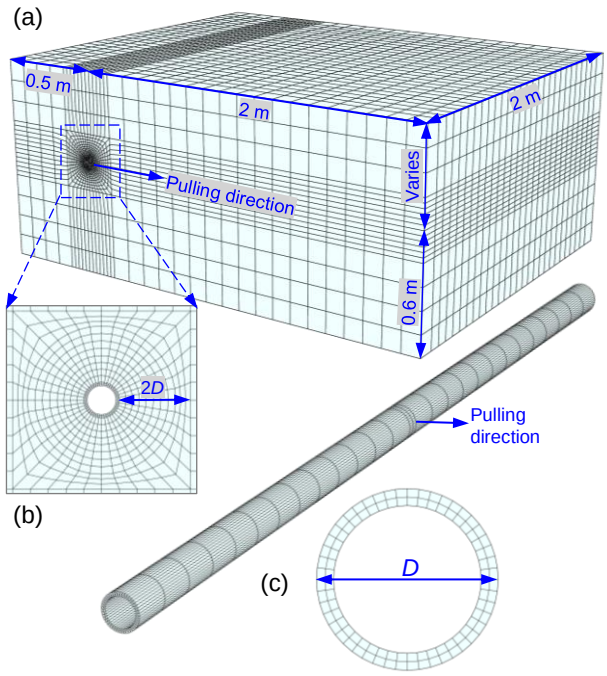

Figure 3. FE model: (a) Soil domain; (b) cross-section near the pipe; (c) MDPE pipe and cross-section

3.3 FE Mesh and Contact Interface

The soil domain was zoned using a structured meshing technique for finer mesh near the pipe where maximum nonlinear deformation was expected. The denser mesh was used within the area, measuring two pipe diameters from the outer surface of the pipe. Larger elements were beyond two times the pipe diameter. A mesh sensitivity analysis was performed to select the optimal mesh for analysis by changing the mesh density only at the zone of interest (the distance of two times pipe diameter from the pipe surface). Figure 4 shows that increasing the number of elements caused the models to converge to a maximum value of pullout force for the cases of Mesh-02 and Mesh-03. Further increase in the element number did not significantly affect the result. Therefore, around 25000–30000 elements were used to model the soil domain. Ninety-six elements were used for the pipe. Pipe thickness was divided into two layers (Figure 3).

A 'general' contact interface with the master-slave contact algorithm was used between the pipe and the soil surfaces. For the slave surface, either it should be a more fine-meshed surface or have a smaller stiffness property. Therefore, the outer pipe surface is assigned to be the master surface, and the soil adjacent to the pipe is considered as the slave surface. For the normal interaction, "hard" contact was defined between the surfaces, which is a nonpenetrating condition. Whereas, for the tangential direction, a friction coefficient, $\mu = \tan\delta$, between the pipe and the soil was defined. The angle of interface shearing resistance, $\delta = f\phi_p'$, is dependent on the soil-pipe interface behavior, including the roughness and hardness of the pipe surface. For polyethylene pipes, the coating-dependent factor, f, was assumed according to ALA (2001). The friction coefficients used for all the tests are shown in Table 2.

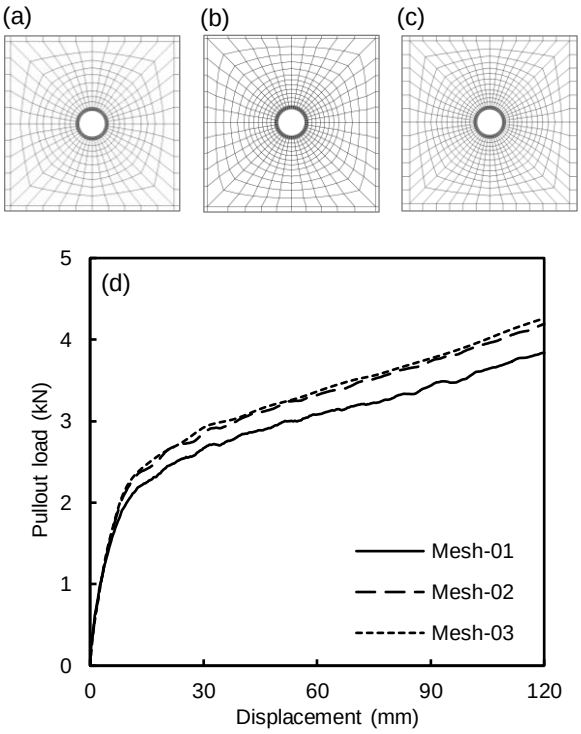

Figure 4. Mesh refinement analyses: (a) Mesh-1 (16896 elements), (b) Mesh-2 (26324 elements), (c) Mesh-3 (29240 elements), (d) Mesh sensitivity effects on pullout response

Table 2. Interface properties of pipe

Contact Parameters	T-1	T-2	T-3	T-4
Coating factor, f	0.6			
Interface friction coefficient, μ	0.47	0.45	0.46	0.45

3.4 Boundary Conditions

The pipe's location with respect to the bottom and side boundaries is sufficiently far to avoid the boundary effects on soil-pipe interaction. The sides of the soil block were restrained horizontally, and the bottom was prevented from movement in all directions. The load was applied uniformly using a displacement boundary condition throughout the circumference at the mid-section, allowing a free vertical movement. The analysis was conducted in two load steps. First, a geostatic analysis was performed under K_0 = 1 condition to establish the initial stress state in the soil, where K_0 is the coefficient of lateral soil pressure at rest. According to Jung et al. (2013), K_0 has no major effect on peak soil lateral resistance. However, values of K_0 less than 1 significantly increase computational time. Next, the pipe was displaced by 120 mm at the midpoint.

The simulations were conducted under nonlinear implicit analysis. The tests were conducted at a reasonably slow rate of 0.5 mm/min, indicating insignificant inertia effects, so quasi-static loading conditions using an implicit solver were applied. The nonlinear geometry (NLGEOM) option was activated in the load-step module to control the mesh distortion at large displacements. Though ALE (Arbitrary Lagrangian-Eulerian) adaptive meshing is a convenient way to control the mesh distortion, it cannot be used for the dynamic implicit solver. The nonlinear geometry activation controlled the element distortion to a great extent and produced satisfactory results. A similar method of analysis was adopted by Almahakeri et al. (2019). All the numerical analyses were verified if the quasi-static condition was satisfied by checking the ratio of kinetic energy (ALLKE) and internal energy (ALLIE).

4 RESULTS

4.1 Force–displacement Response

The predicted FE results and recorded test measurements in terms of force–displacement relations are shown in Figure 5. It appears the proposed method of analysis reasonably predicted the observed test results. Particularly, the ultimate values of pullout forces and the initial elastic portion of the force–displacement curves correlate quite well with the test results. For Tests T-2 to T-4, the peak pullout force continues to increase up to the displacement of 120 mm, (the maximum displacement applied during the tests), indicating that the peak soil resistance was not reached in these tests.

However, in Test T-1 (42.2-mm pipe with a burial depth of 337 mm), peak pullout resistance was observed at around 60 mm of mid-span displacement, which decreased with further pipe displacements. In this test, cracks on the soil surface were observed, indicating that the peak soil resistance was reached during the test with a shallow burial depth (i.e., 337 mm) (Sinha et al., 2021). The FE model could not simulate this post-peak strain-softening behavior due to the limitation of the numerical technique. The peak pullout resistance is the primary focus of this current study, and the post-peak responses are not simulated in the FE analysis.

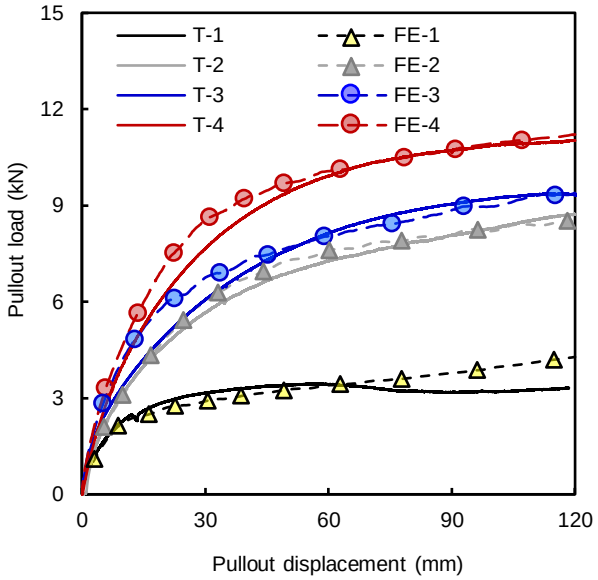

Figure 5. Simulation of load–displacement response

4.2 Strain Response

Figure 6 shows comparisons of axial strains measured during the Tests T1 with those found using numerical analysis. The other test results are not included here for the sake of brevity. Due to the pipe's longitudinal bending, stresses were measured at four locations along its length at the pipe springlines marked in Figure 6 (a). According to Brachman (1999) and Dhar and Moore (2001), the adhesive for mounting the strain gauges on the pipe increases the stiffness property of the pipe wall, which means the measured strains can be less than the actual strain. Thus, measured strains were corrected by a correction factor of 0.7 (Reza and Dhar, 2021).

In all the tests, the maximum strain was measured near the midspan of the pipe, while the other strain gauge measurements were significantly lower. It is found that the maximum axial strain near the pullout location is higher for the shallow buried pipe, although the pulling force was the minimum. Note that two oppositely placed strain gauges, S.G-1 and S.G-2, measured compressive and tensile strains simultaneously, proving a curvature change of the pipe within 450 mm from the loading point. This change in curvature was visible after the test when the pipe was exposed. In the case of the other tests, i.e., Test T-2, the strain reached a maximum value and then reduced due to the development of local buckling observed in the test. For the tests T-3 and T-4, bending strains were comparatively higher than the other two due to the diameter effect. Although these three tests are not included here, the FE findings show reasonable agreement with the test strain values. This shows that the test conditions can be simulated effectively using this FE modeling technique.

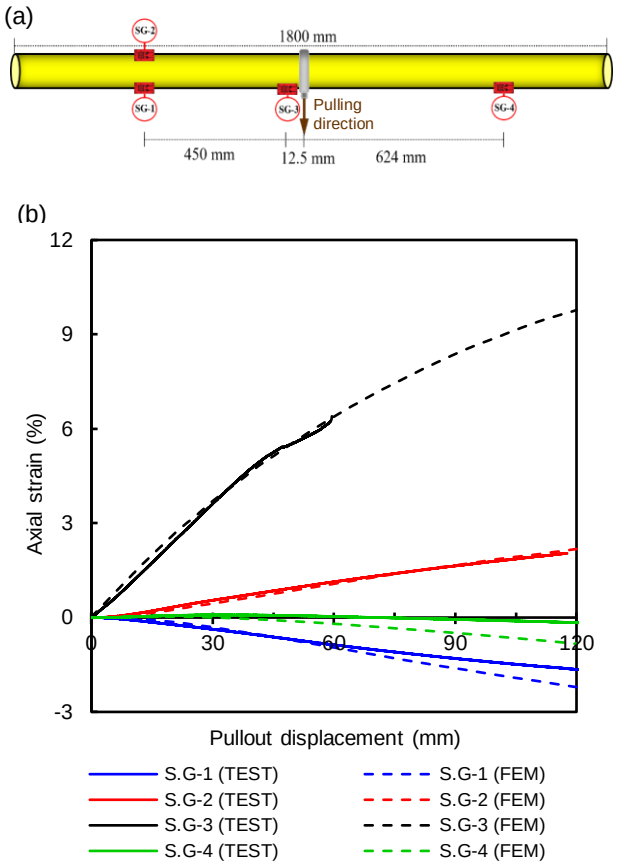

Figure 6. Pipe wall strain comparisons (a) Positions of the strain gauges (S.G); and (b) Test T-1

5 INVESTIGATION OF PIPE RESPONSES

5.1 Strain Distribution along the Length

During the tests, the strains were measured at discrete points, providing only a limited idea of the strain distribution over the pipe length. Figure 7 depicts the numerically calculated axial strain variation over the length of the pipe, and the corresponding measured values. Axial strains were relatively high near the pulling point and progressively reduced to a minimum towards two ends of the pipe. The high axial strains toward the pulling point are associated with higher relative movement between the soil and pipe elements, which may cause full development of the interface shear strength. The existence of a 25 mm grip during the test that was modelled to be uniformly loaded may be responsible for the drop of peak strain at the midpoint of the pipe. The strains correspond to three pulling forces, one within linear (5 mm displacement) and the others within the nonlinear ranges (60 mm, 120 mm displacement) of load-displacement response observed during the tests (i.e., Figure 5), were compared in the figure. For Test T-1, the comparison shows considerable agreement between experimentally measured strains and computational estimates for the linear load-displacement relation. However, the numerical solutions underestimate the values at the high strain zone. The discrepancies might be due to the limitations of the conventional Mohr-Coulomb model to capture the highly nonlinear responses of soil, particularly the post-peak degradation of soil strength. Another explanation for the inconsistency is limitations associated with test conditions. For instance, the soil around the pipe could not be adequately compacted due to the installment of the sensors.

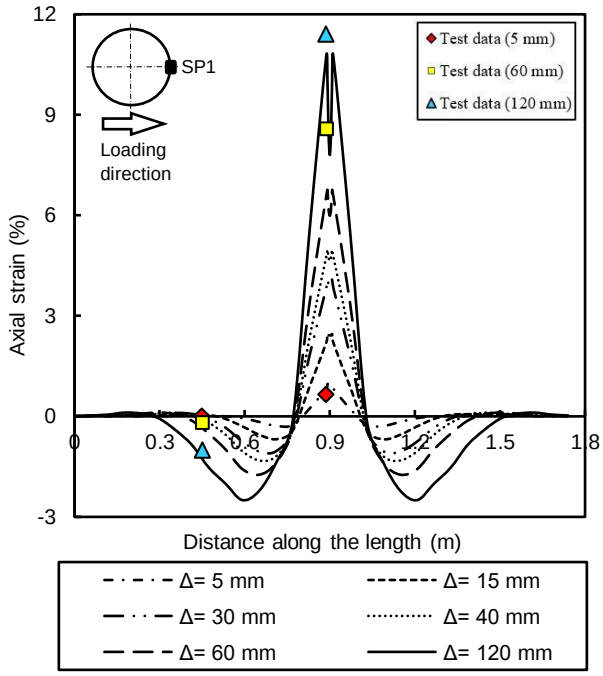

Figure 7. Lengthwise distribution of axial strains along the spring line at the pulling direction (SP1) during Test T1.

5.2 Lengthwise Variation of Normal Stress

To better understand the complex load transfer mechanism of the flexible pipe, the authors studied the distribution of normal stresses along the length of the pipe using FE analysis. The distributions of normal stresses around the pipe circumference at different locations along the pipe length were obtained from FE analysis. Then, the normal stresses averaged over the pipe circumference were plotted along the pipe length for different pipe displacements in Test T-1, as shown in Figure 8. The magnitude of the stresses is maximum at the pulling point at 60 mm of pipe displacement. Then, the stress at this point decreases for further pulling displacements. However, the stresses away from the pulling nodes are almost the same at higher pipe displacements. During the test T-1, the maximum lateral load was obtained at 60 mm of pipe displacement, and then the soil resistance was reduced with further displacement.

After the test, soil surface crack was also observed in Test T-1, which had a shallow burial depth of 337 mm. At this shallower depth, the soil failure mechanism due to

lateral pipe movements was the overbreak of the soil at the surface, reducing the normal stress on the pipe.

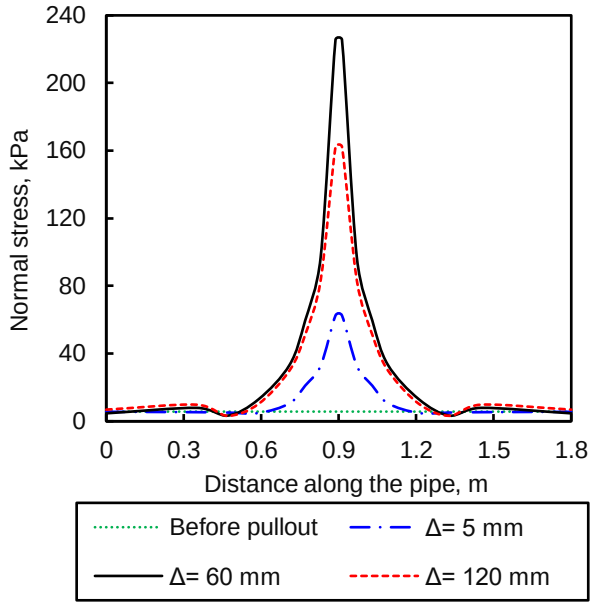

Figure 8. Normal stress distribution along the pipe length for Test T-1

6 CONCLUSIONS

The current study presents a 3D FE modeling approach to simulate the full-scale tests conducted on buried MDPE pipes exposed to lateral earth movements. The Mohr-Coulomb constitutive model was used for the soil material with stress-dependent values of soil modulus, friction angle and dilation angle. The numerical computations were compared to experimental findings and concluded with the following key findings:

- Applying the dynamic implicit solver with nonlinear geometry control has successfully prevented excessive mesh distortion due to large deformation. Without regard for the complexity of the dynamic explicit application, this approach may effectively evaluate the loading scenario with the minimum element distortion and the optimum computational time.
- The conventional Mohr-Coulomb model can reasonably predict the mechanical response of the pipeline to ground deformation up to the peak load behavior. As the peak load behavior is the main concern of the study, the incapability of the model to predict the post-peak behavior has not been considered.
- This modeling approach can successfully simulate the strain data from the tests. The maximum strain happens to be near the loading point and gradually diminishes toward the ends of the pipe.

7 ACKNOWLEDGEMENTS

The authors gratefully acknowledge the financial and/or in-kind support provided by the Natural Science and Engineering Research Council of Canada through its Discovery and Collaborative Research and Development Grant programs, FortisBC Energy Inc., and WSP Canada Inc.

8 REFERENCES

ALA (American Lifelines Alliance). 2001. Guidelines for the design of buried steel pipe, Reston, VA, USA: ASCE.

Alarifi, H., Mohamad, H., Nordin, N. F., Yusoff, M., Rafindadi, A. D. U. and Widjaja, B. 2021. A Large-Scale Model of Lateral Pressure on a Buried Pipeline in Medium Dense Sand. *Applied Sciences*, 11(12): 5554.

Almahakeri, M., Moore, I.D. and Fam, A., 2012. The flexural behavior of buried steel and composite pipes pulled relative to dense sand: Experimental and numerical investigation. In Proc., *9th International Pipeline Conference*, American Society of Mechanical Engineers Digital Collection, pp: 97-105.

Almahakeri, M., Fam, A. and Moore, I.D., 2014. Experimental investigation of longitudinal bending of buried steel pipes pulled through dense sand. *Journal of Pipeline Systems Engineering and Practice*, 5(2):04013014.

Almahakeri, M., Moore, I. D. and Fam, A. 2016. Numerical study of longitudinal bending in buried GFRP pipes subjected to lateral earth movements. *Journal of Pipeline Systems Engineering and Practice*, 8(1): 4016012.

Almahakeri, M., Moore, I. D. and Fam, A. 2019. Numerical techniques for design calculations of longitudinal bending in buried steel pipes subjected to lateral Earth movements. *Royal Society Open Science*, 6(7).

Ansari, Y., Kouretzis, G. and Sloan, S. W. 2018. Development of a prototype for modeling soil–pipe interaction and its application for predicting uplift resistance to buried pipe movements in sand. *Canadian Geotechnical Journal*, 55(10): 1451-1474.

Audibert, J. M. E., and Nyman, K. J. (1977). Soil restraint against horizontal motion of pipes. Journal of the Geotechnical Engineering Division, 103(10), 1119–1142.

Bolton, M. D. 1986. The strength and dilatancy of sands, *Géotechnique*, 36(1): 65–78.

Brachman, R. W. I. 1999. Structural performance of leachete collection pipes. Ph.D. thesis, Dept. of Civil and Environmental Engineering, Univ. of Western Ontario.

Dassault Systems. 2019. ABAQUS/CAE user's guide. Providence, RI: Dassault Systemes Simulia.

Das, B. M. and Seeley, G. R. 1975. Load-displacement relationship for vertical anchor plates, *Journal of Geotechnical and Geoenvironmental Engineering*. 101(7): 711-715.

Daiyan, N., Kenny, S., Phillips, R. and Popescu, R. 2010. Numerical investigation of oblique pipeline/soil interaction in sand. In Proc., *8th International Pipeline Conference*, Calgary, Alberta, Canada. September 27–October 1, Vol. 2, 2010. pp. 157-164.

Das, S. and Dhar, A. S. 2021. Nonlinear time-dependent mechanical behavior of medium-density polyethylene pipe material. *Journal of Materials in Civil Engineering*, 33(5): 04021068.

Dhar, A. S., and I. D. Moore. 2001. "Liner buckling in profiled polyethylene pipes." Geosynth. Int. 8 (4): 303–326.

Guo, P. J. and Stolle, D. F. E. 2005. Lateral pipe–soil interaction in sand with reference to scale effect. *Journal of Geotechnical and Geoenvironmental Engineering*, 131(3): 338-349.

Hansen, J. B. 1961. The ultimate resistance of rigid piles against transversal forces. Bulletin 12, Danish Geotech. Institute, 1–9.

Hsu, T.-W. 1993. Rate effect on lateral soil restraint of pipelines. Soils and Foundations, 33(4): 159–169.

Jung, J., T. O'Rourke, and N. Olson. 2013. "Uplift soil–pipe interaction in granular soil." Can. Geotech. J. 50 (7): 744–753.

Konuk, I., Phillips, R., Hurley, S., and Paulin, M. J. 1999. Preliminary ovalisation of buried pipeline subjected to lateral loading. In Proc., *Offshore Mechanics and Arctic Engineering (OMAE)*, St. John's, NL.

Kulhawy, F.H., and Mayne, P.W. 1990. Manual on estimating soil properties for foundation design. Report EPRI-EL 6800, Electric Power Research Institute, Palo Alto. pp. 306.

Lings, M. L., and Dietz, M. S. 2004. "An improved direct shear apparatus for sand." Geotechnique, 54(4):245−256.

Murray, E. J. and Geddes, J. D. 1989. Resistance of passive inclined anchors in cohesionless medium, G'eotechnique, 39(3): 417–431.

Neely, W. J., Stuart, J. C. and Graham, J. 1973. Failure loads of vertical anchor plates in sand, *Journal of Soil Mechanics & Foundations*, Div 99 (Proc. Paper 9980).

Ovesen, N. K. 1964. Anchor slabs, calculation methods and model tests, Bulletin 16, 39.

Ovesen, N. K. and Strømann, H. 1972. Design method for vertical anchor slabs in sand, in 'Performance of earth and earth-supported structures', ASCE, p. 1481.

Popescu, R., Guo, P. and Nobahar, A. 2001. 3D finite element analysis of pipe/soil interaction. Final Report for Geological Survey of Canada, Chevron Corp. and Petro Canada.

Reza, A. and Dhar, A. S. 2021. Axial Pullout Behavior of Buried Medium-Density Polyethylene Gas Distribution Pipes. *International Journal of Geomechanics*, 21(7): 04021120.

Robert, D. J., Rajeev, P., Kodikara, J. and Rajani, B. 2016. Equation to predict maximum pipe stress incorporating internal and external loadings on buried pipes. *Canadian Geotechnical Journal*, 53(8): 1315-1331.

Roy, K., Hawlader, B., Kenny, S. and Moore, I. 2015. Finite element modeling of lateral pipeline–soil interactions in dense sand. *Canadian Geotechnical Journal*, 53(3): 490-504.

Roy, K., Hawlader, B., Kenny, S. and Moore, I. 2018. Lateral resistance of pipes and strip anchors buried in dense sand. *Canadian Geotechnical Journal*, 55(12): 1812-1823.

Sinha. 2021. Lateral ground movement effects near connection of medium density polyethylene gas distribution pipes. Master's thesis, Memorial University of Newfoundland.

Sinha, T. Dhar, A.S., Weerasekara, L. and Rahman, M. 2021. Effects of lateral ground movements on MDPE gas distribution pipes and branches, In Proc., *74th Canadian Geotechnical Conference*, GeoNiagara 2021, Sept. 26-29, Niagara,ON.

Suleiman, M. T., and Coree, B. J. 2004. Constitutive model for high density polyethylene material: systematic approach. *Journal of Materials in Civil Engineering*, 16(6): 511-515.

Trautmann, C. H. 1983. Behavior of pipe in dry sand under lateral and uplift loading, PhD thesis, Cornell Univ., Ithaca, NY.

Xie, X., Symans, M. D., O'Rourke, M. J., Abdoun, T. H., O'Rourke, T. D., Palmer, M. C. and Stewart, H. E. 2013. Numerical modeling of buried HDPE pipelines subjected to normal faulting: a case study. *Earthquake Spectra*, 29(2): 609-632.

Yimsiri, S., Soga, K., Yoshizaki, K., Dasari, G. R. and O'Rourke, T. D. 2004. Lateral and upward soil-pipeline interactions in sand for deep embedment conditions. *Journal of geotechnical and geoenvironmental engineering*, 130(8): 830-842.